

Supporting for

## **Orthometric Multicolor Encoded Hybridization Chain Reaction Amplifiers for Multiplexed MicroRNAs Profiling in Living Cells**

Wei Wei,<sup>a, b, c</sup> Yiyi Zhang,<sup>b</sup> Fan Yang,<sup>b</sup> Liping Zhou,<sup>b</sup> Yufan Zhang,<sup>a, b</sup> Yeyu Wang,<sup>a, b, c</sup> Shuangshuang Yang,<sup>a, b</sup> Jinze Li,<sup>a, b</sup> and Haifeng Dong\*,<sup>a, b</sup>

---

<sup>a</sup> Marshall Laboratory of Biomedical Engineering, Research Center for Biosensor and Nanotheranostic, School of Biomedical Engineering, Shenzhen University, 3688 Nanhai Road, Shenzhen, 518060, Guangdong, China

<sup>b</sup> Beijing Key Laboratory for Bioengineering and Sensing Technology, School of Chemistry and Bioengineering, University of Science and Technology Beijing, 30 Xueyuan Road, 100083, Beijing, China.

<sup>c</sup> Beijing Yaogen Biotechnology Co. Ltd, 26 Yongwangxi Road, 102609, Beijing, China

\*E-mail: [hfdong@ustb.edu.cn](mailto:hfdong@ustb.edu.cn), [hfdong@szu.edu.cn](mailto:hfdong@szu.edu.cn)

<b>Experimental Section</b> .....	4
<b>Materials and Reagents</b> .....	4
<b>Equipment</b> .....	4
<b>Quantification of the HCR hairpin probes on DMSN</b> .....	5
<b>Gel Electrophoresis</b> .....	5
<b>Cytotoxicity</b> .....	5
<b>Intracellular ROS/Hypoxia assay</b> .....	5
<b>Mitochondrial membrane potential assay</b> .....	5
<b>Western Blot</b> .....	6
<b>Apoptosis analysis</b> .....	6
<b>Autophagy assay</b> .....	6
<b>QPCR</b> .....	6
<b>Supplementary Figures</b> .....	7
<b>Fig.S1</b> . Schematic indication for the logical orthometric combination of the multi-HCR assembles and recognition way. ....	7
<b>Fig.S2</b> . The self-dimer structure of HCR hairpins for miRNA-155. ....	8
<b>Fig.S3</b> . A control experiment in Fig.1a where the control hairpin sequences were intact as they were missing in the toehold part. ....	8
<b>Fig.S4</b> . Representative native-PAGE electrophoresis of miRNA-155-triggered HCR reaction. ....	9
<b>Fig.S5</b> . FL analysis of the multi-HCR system in response to different concentrations (10 pM-100 nM) of miRNA-155. ....	9
<b>Fig.S6</b> . Multi-HCR encoded barcodes for Fig.1c based on 3 dyes (AF488, AF594, AF647) labeled hairpins in response to target miRNA-155. ....	10
<b>Fig.S7</b> . 4-colored fluorochromes combination and sequence extension for miRNA-155 multi-HCR encoding chain assemble. ....	11
<b>Fig.S8</b> . Excitation curve of different fluorescent HCR hairpins. ....	12
<b>Fig.S9</b> . Cell viability assay by CCK8 test. DMSN@H for different times. ....	13
<b>Fig.S10</b> . The different pHs effected on the size and FL of DMSN@H. ....	13
<b>Fig.S11</b> . Hypoxia-induced Mito-ER stress and apoptosis/autophagy process. ....	14
<b>Fig.S12</b> . Fluorochrome combinations for 8 different miRNAs detection. ....	15
<b>Fig.S13</b> . Multi-HCR barcodes extension sequences for the 8 miRNAs detection. ....	16
<b>Fig.S14</b> . Representative native-PAGE electrophoresis for HCR reactions. ....	17
<b>Fig.S15</b> . Multiplexed miRNAs detection separately in hypoxia adaptive signal pathway. ....	18
<b>Fig.S16</b> . Representative CLSM analysis by channels for decoding the multi-HCR barcodes worked simultaneously in living cells and compared the FL intensity changes in normal and hypoxia treated Hct116 cells. ....	19
<b>Supplementary Tables</b> .....	20
<b>Table S1</b> . Sequences used for feasibility analysis of assembling 15 kinds of Multi-HCR barcodes in this work. ....	20
<b>Table S2</b> . Multi-HCR chain composition for FL detection in liquid. ....	21
<b>Table S3</b> . DMSN@H composition used for CLSM detection of miRNA-155 in living	

cells. ....	22
<b>Table S4.</b> 8 miRNAs' functions in hypoxia-induced signaling pathways reported by former research. ....	23
<b>Table S5.</b> Sequences used for 8 miRNAs array analysis in the hypoxia-induced intracellular process. ....	24
<b>Table S6. Abbreviation List.</b>	
<b>Reference</b> .....	26

## Experimental Section

### Materials and Reagents.

Cetyltrimethylammoniumtosylate (CTAT), tetraethyl orthosilicate (TEOS), triethanolamine (TEA), sodium salicylate (NaSal), dimethyl sulfoxide (DMSO), 3-mercaptopropyltrimethoxysilane (MPTES), bis[3-(triethoxysilyl)propyl]tetrasulfide (BTESPT), Tris(2-carboxyethyl)phosphine (TCEP), mercaptoethanol (ME), 2-[4-(2-hydroxyethyl)-1-piperazinyl] ethanesulfonic acid buffer solution (HEPES), CCK8 were brought from Sigma-Aldrich (Shanghai, China). L-buthionine sulfoximine (BSO) was purchased from Shanghai Yuanye Bio-Technology Co., Ltd (Shanghai, China). Phosphate-buffered saline (PBS, pH 7.4), gelred, Dulbecco's Modified Eagle's medium (DMEM), penicillin-streptomycin, trypsin-EDTA, and JC-10 mitochondrial membrane potential assay kit were purchased from Solarbio Science & Technology Co., Ltd. (Beijing, China). Opti-MEM and fetal bovine serum (FBS) were purchased from Gibco Life Technologies (AG, Switzerland). MiRcute miRNA isolation kit, miRcute plus miRNA first-strand cDNA synthesis kit, and miRcute plus miRNA qPCR Detection Kit (SYBR Green) were purchased from Tiangen Biotech (Beijing, China). A cell endoplasmic reticulum isolation kit was brought from Beijing Baiaolaibo Technology Co., Ltd (Beijing, China). Fluo-4 AM, Caspase 3 activity assay kit, autophagy staining assay kit with MDC, Earle's Balanced Salt Solution (EBSS), Annexin V-FITC apoptosis detection kit, and all the antibodies were brought from Beyotime Biotechnology (Shanghai, China). Cyto-ID Hypoxia/Oxidative stress detection kit were purchased from Enzo Life Sciences, Inc. (New York, USA). The ultrapure water (ddH<sub>2</sub>O, 18 MΩ.cm) was obtained from a water purification system (Millipore, USA). All chemicals used in this study were analytical reagent grade and used without further purification. ALL HCR hairpins and other DNA sequences were ordered from Sangon Biological Engineering Technology & Services (Shanghai, China). The FL dyes (AF405, AF488, AF594, AF647) contain a succinimidyl ester to link with the NH<sub>2</sub>-C6-dT in the DNA oligo by amidation reaction, forming amido bonds.

### Equipment.

The morphologies of the DMSNs and HCR barcodes were acquired with a transmission electron microscope (TEM, HT7700, Hitachi, Japan). Gel electrophoresis and western blot images were captured by a gel-imaging system (UVItec FireReader, UK). The fluorescence electrophoresis images were taken by a fluorescent scanner (4800Multi, Tanon, China). The fluorescence (FL) spectra were measured with an FL spectrophotometer (F-7000, Hitachi, Japan). UV-Visible (UV-Vis) absorption was measured with a spectrophotometer (UV-1800, Shimadzu, Japan). Cytotoxicity test was recorded by Anthos 2010 microplate reader (Biochrom Ltd., Cambridge CB4 0FJ, England). The apoptosis assay used a flow cytometry machine (FCM, NovoCyte, Agilent, USA). The data was analyzed using the NovoExpress RUO software. The confocal laser scanning microscopy (CLSM) images were acquired on an inverted confocal microscope (TCS SP5, Leica,

Germany). AnaerPack™-Anaero and AnaerPack™-MicroAero boxes (2.5 L , Mitsubishi, Japan) were used to hypoxia cell culture. O<sub>2</sub> Quickstick Oxygen Analyzer (K-100A, Kailu electronic, China) was used to monitor the O<sub>2</sub> content in the chamber.

#### **Quantification of the HCR hairpin probes on DMSN.**

To test the amount of the HCR hairpin on the DMSN-SH vector, HCR DNA probes labeled with carboxyfluorescein (FAM) were first adsorbed to DMSN-SH. 0.5 mL of the obtained DMSN@H (1 mg/mL) was treated with 10  $\mu$ L ME (20 mM) overnight at room temperature<sup>1</sup>. Then the solution was centrifuged, and the supernatant was collected for fluorescence measurement. The amount of the DNA probe modified on the DMSN surface was quantified by a companion with the standard curve of the DNA probe.

#### **Gel Electrophoresis.**

HCR hairpins (H1, H2, H3, H4) and miRNA were diluted to 2  $\mu$ M and incubated at 37 °C for 2 h. Then they were loaded into a native 12 % polyacrylamide gel; the running was performed in 1x TAE buffer at 150V for 1.5 h. The gels were merged in gelred buffer for 10 min before imaging using a UV imager system (UVItec FireReader, UK).

Fluorescent DNA image was captured by a fluorescent scanner (Tanon, China) with the excitation laser sources and emission filters were as follows<sup>2</sup>: 473 nm laser with 535nm and 10 nm bandpass filter (for AF488), 560 nm laser with 590 nm and 10 nm bandpass filter (for AF594), and 635 nm laser with 665 nm long-pass filter (for AF 647).

#### **Cytotoxicity.**

The biosafety of the multi-HCR barcodes was assessed using a standard CCK-8 assay. A density of  $1 \times 10^4$  Hct116 cells was cultured in 96-well plates at 37 °C at per well for 24 h. Different concentrations of multi-HCR (10, 25, 50, 100, 200  $\mu$ g/mL) were treated with Hct116 cells for 4 h, 12 h, 24 h, 36 h, and 48 h. Subsequently, the cells were changed with 100  $\mu$ L new DMEM culture (pH 7.4, 10 mM), and 10  $\mu$ L CCK-8 solution was added into each well. After incubating the absorbance was recorded at 492 nm using an Anthos 2010 microplate reader.

#### **Intracellular ROS/Hypoxia assay.**

The intracellular ROS and hypoxia production was assayed by a hypoxia/oxidative stress detection kit<sup>3</sup>. Hypoxia/oxidative stress detection probes were added and incubated with the cells ( $1 \times 10^5$ /well) for 5 min and observed using CLSM. The green ROS and red hypoxic fluorescence signals were recorded with an excitation wavelength of 488 nm and 561 nm by CLSM, respectively.

#### **Mitochondrial membrane potential assay.**

Mitochondrial membrane potential detection was performed according to the producer's manuscript. Briefly, the CCCP (10  $\mu$ M) was used as a positive control. It treated the cell for 20 min to eliminate the mitochondrial membrane potential, resulting in green color. Then, differently treated group cells in confocal dishes were reacted with 1 mL JC-10 working buffer for 20 min at 37 °C and washed twice with

icy JC-10 dying buffer. Then the cells were detected with CLSM. When detecting JC-10 monomer, the excitation light and emission light was set as 488 nm and 530 nm, respectively; when detecting JC-10 polymer, the excitation light was set at 525nm and the emission light at 590nm.

#### **Western Blot.**

Firstly, 10% SDS-PAGE electrophoresis separated the protein from different treatment groups. Then, the proteins in the gel were transferred into the PVDF membrane and sequentially incubated with specific primary antibodies. HRP labeled second antibodies overnight under a gentle shake. Finally, pictures were captured by a chemiluminescence imager (UVItec FireReader, UK).

#### **Apoptosis analysis.**

Both FCM and CLSM methods performed apoptosis detection. For the CLSM experiment,  $1 \times 10^4$  Hct116 cells were seeded in a confocal dish. After the normal and hypoxia treatment mentioned above, the apoptosis maker of Caspase 3 was analyzed using a Caspase 3 Activity Assay Kit. For the FCM experiment,  $1 \times 10^5$  Hct116 cells were seeded in the 6-well plates. After the normal and hypoxia treatment, the cells were assayed using an Annexin V-FITC apoptosis detection kit following the manufacturer's protocol and determined using flow cytometry.

#### **Autophagy assay.**

$1 \times 10^4$  Hct116 cells were seeded in a confocal dish. the monodansylcadaverine (MDC) autophagy probe was incubated with the cells for 30 min at 37 °C, and an EBSS-treated cell was used as the positive control. The CLSM images were taken at the excitation of 405 nm and the emission light of 510-540 nm band.

#### **QPCR.**

Total RNA was extracted from cell lysates according to the manufacturer's protocol. A miRcute Plus miRNA First-Strand cDNA Synthesis Kit (Tiangen Biotech, Beijing, China) and a miRcute Plus miRNA qPCR Detection Kit (Tiangen Biotech, Beijing, China) were used for miRNAs analysis. U6 was used as the housekeeping gene, and the relative miRNA levels or U6 quantity in each fraction were expressed as  $2^{-\Delta Ct}$  value (2 to the power of negative  $\Delta Ct$ ). All runnings followed the MIQE rules<sup>4</sup>. Each data point was run in triplicate, and data were acquired using 7500 Software (version 2.3, Applied Biosystems, USA). Levels of miRNA expression in the different groups were evaluated using unpaired Student's *t*-test and Benjamin-Hochberg multiple testing to correct *p* values<sup>5</sup>.

SUPPLEMENTARY FIGURES

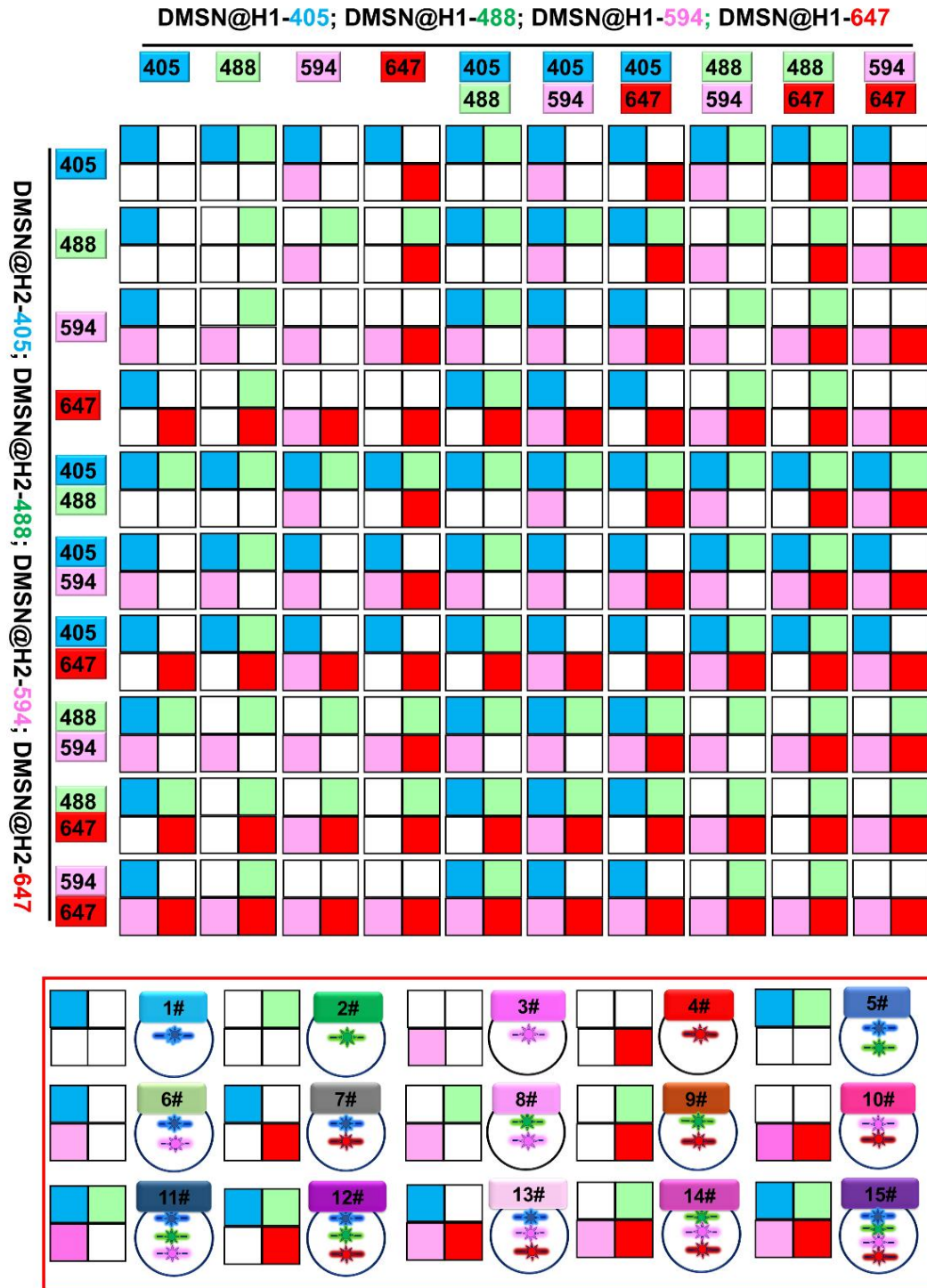


**Fig.S1.** Schematic indication for the logical orthometric combination of the multi-HCR assemblies and recognition way. The combinations in the down red box indicate the associated barcodes in Scheme 1.

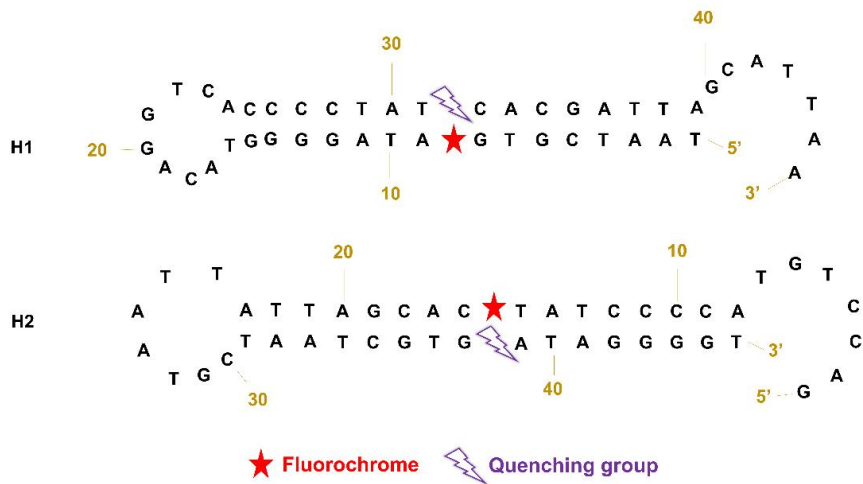


**Fig.S2.** The self-dimer structure of HCR hairpins for miRNA-155.

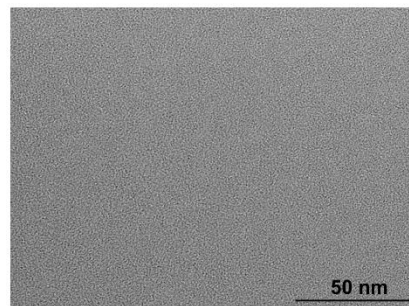


**Fig.S3.** In a control experiment in Fig.1a, the control hairpin sequences were intact, as they were missing in the toehold part.

miRNA-155-H1': TAATCGTGATAGGGGTACAGGTCACCCCTATCACGATTA;

miRNA-155-H2': ACCCCTATCACGATTATTAATGCTAATCGTGATAGGGGT



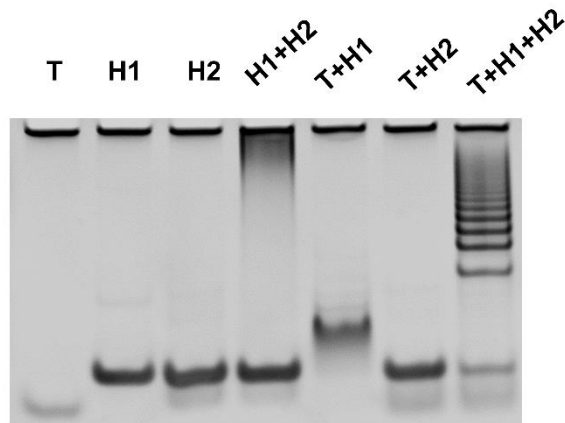


**Fig.S4.** Representative native-PAGE electrophoresis of miRNA-155-triggered HCR reaction. T: target miRNA-155; H1: Hairpin 1; H2: Hairpin 2. The loading concentration of each lane was 2  $\mu$ M.

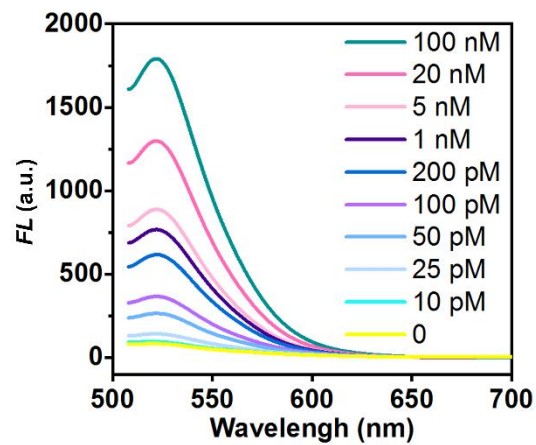


**Fig.S5.** FL analysis of the multi-HCR system in response to different concentrations (10 pM-100 nM) of miRNA-155. The FAM FL was excited by 488 nm.

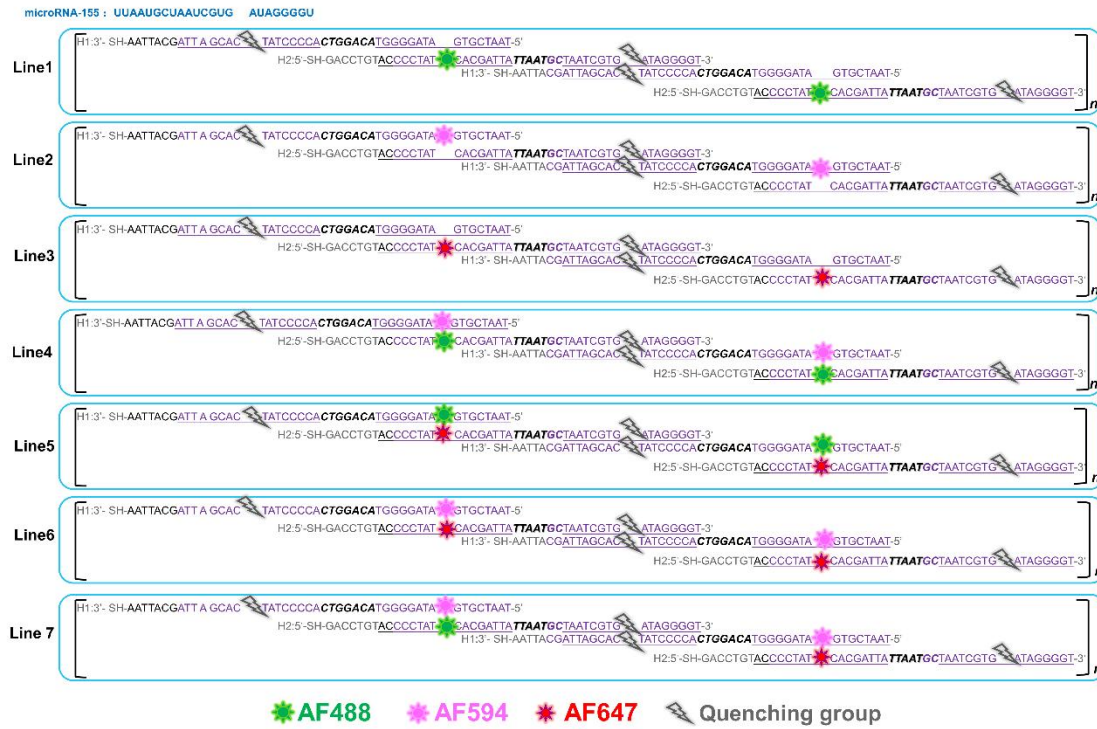


**Fig.S6.** Multi-HCR encoded barcodes for Fig.1c based on three dyes (AF488, AF594, AF647) labeled hairpins in response to target miRNA-155.

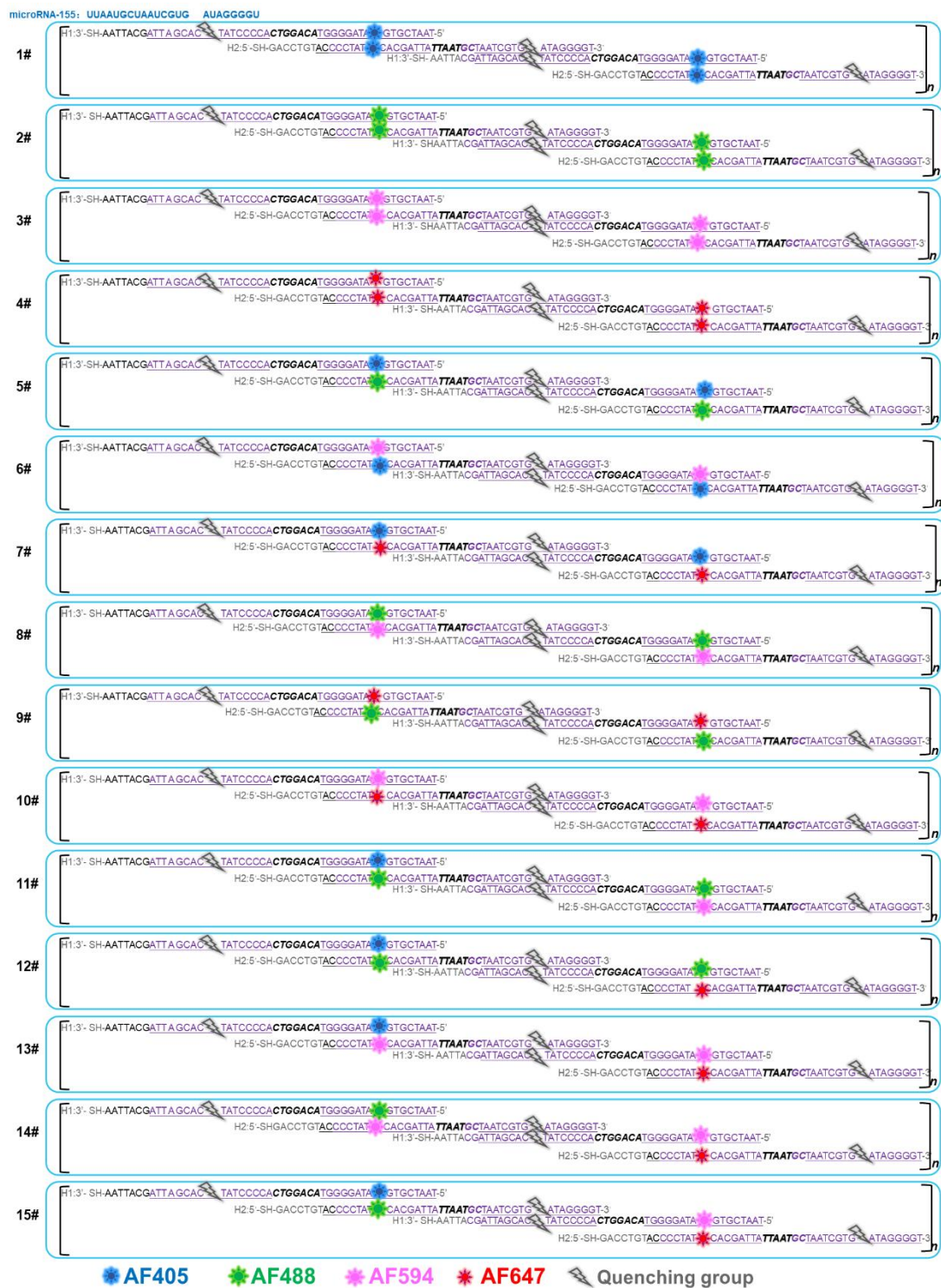
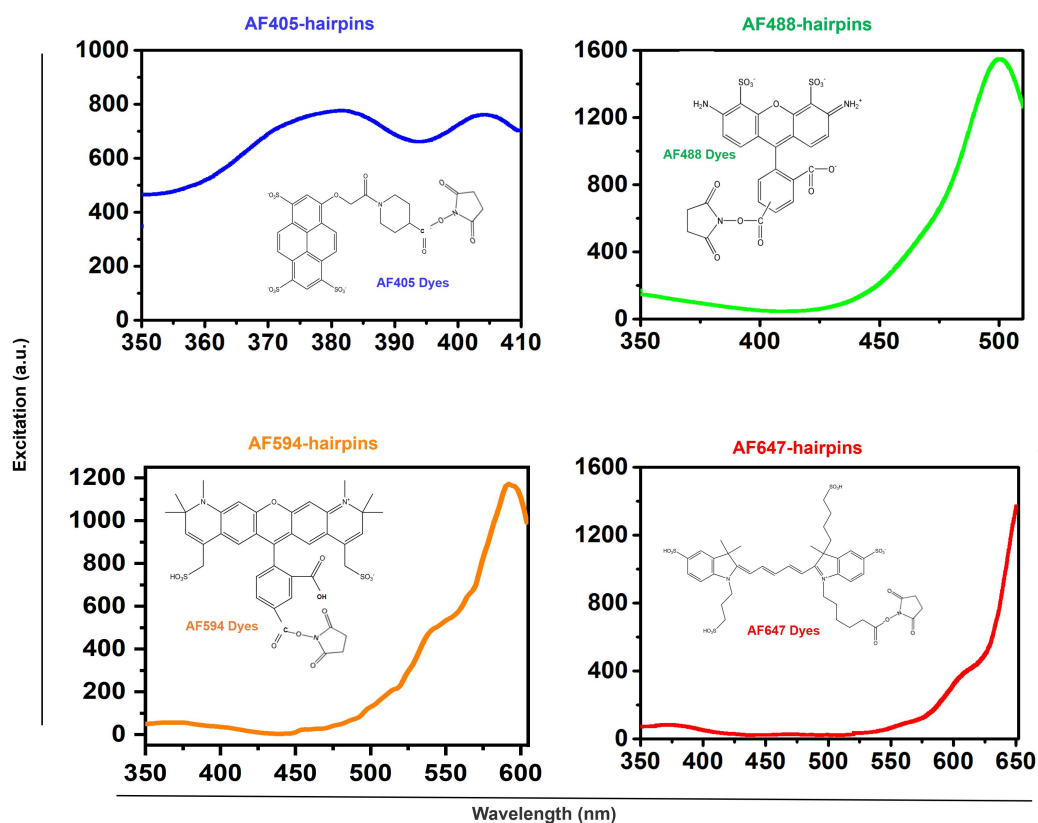
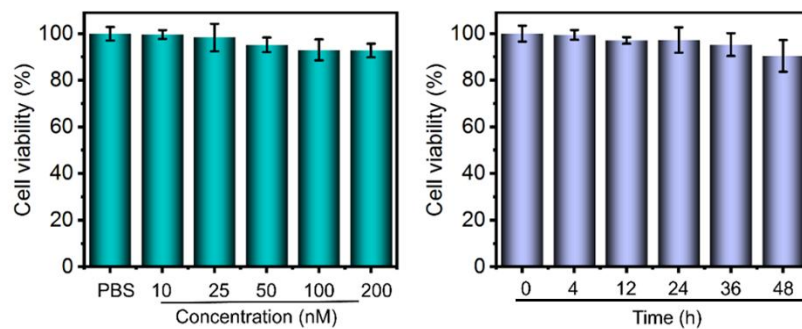


Fig.S7. 4-colored fluorochromes combination and sequence extension for miRNA-155 multi-HCR encoding chain assemble.



**Fig.S8.** Excitation curve of different fluorescent HCR hairpins. The FL dyes structure of AF405, AF488, AF594, and AF647 was illustrated in the images. All the dyes contain a succinimidyl ester to link with the NH<sub>2</sub>-C6-dT in the DNA oligo by amidation reaction, forming an amido bond.



**Fig.S9.** Cell viability assay by CCK8 test. (a) Cells were treated with different concentrations (10-200 nM) of DMSN@H. (b) cells were incubated with 100  $\mu\text{g}/\text{mL}$  DMSN@H for different times (0-48 h). The error bars indicate mean  $\pm$ SD (n=5).

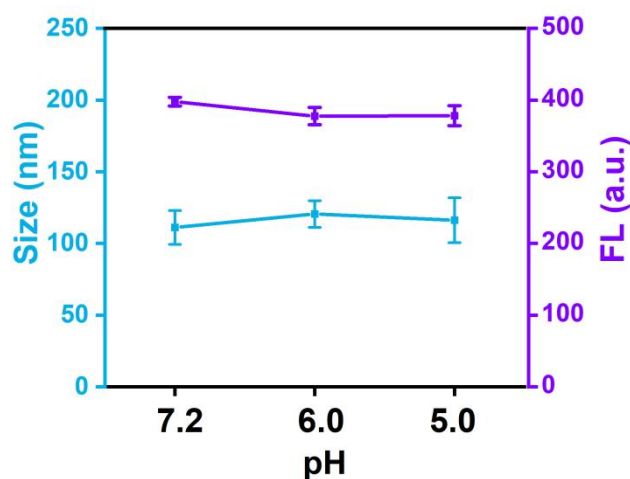


**Fig.S10.** The different pHs affected the size and FL of DMSN@H. The target miRNA concentration was 100 nM in pH 7.2, pH 6.0, and pH 5.0 PBS buffers. The error bars indicate mean  $\pm$ SD (n=3).

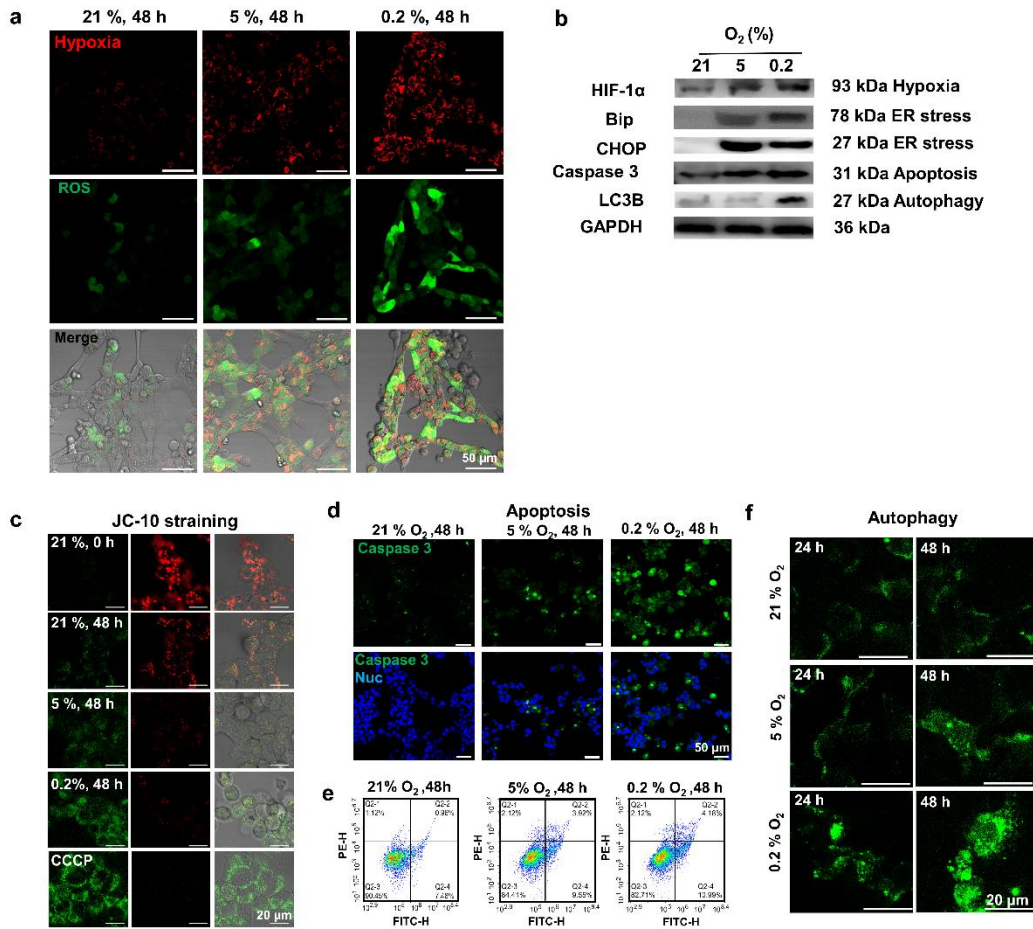


**Fig.S11.** Hypoxia-induced Mito-ER stress and apoptosis/autophagy process. (a) Representative CLSM images for hypoxia-induced ROS production. (b) Western blot assay for the classic protein markers in cellular hypoxia adaptive alteration. It showed the enhanced expression of hypoxia-inducible factor-1 $\alpha$  (HIF-1 $\alpha$ )<sup>6</sup>, ER-stress markers of immunoglobulin heavy chain binding protein in pre-B cells (Bip,) and C/EBP-homologous protein (CHOP)<sup>7</sup>, and apoptosis and autophagy markers of Caspase 3<sup>8</sup> and light chain 3 (LC3B)<sup>9</sup> during the low oxygenation process. (c) Representative CLSM images for the mitochondrial membrane potential assay. It showed an increased JC-10 monomer with green fluorescent under hypoxia, indicating mitochondrial stress (Mito-stress) and early apoptosis (d) Representative CLSM images and (e) FCM test for apoptosis assay. (f) Representative CLSM images for hypoxia-induced autophagy. It showed prominent green autophagy spots in 0.2 % O<sub>2</sub> treatment for 48 h.



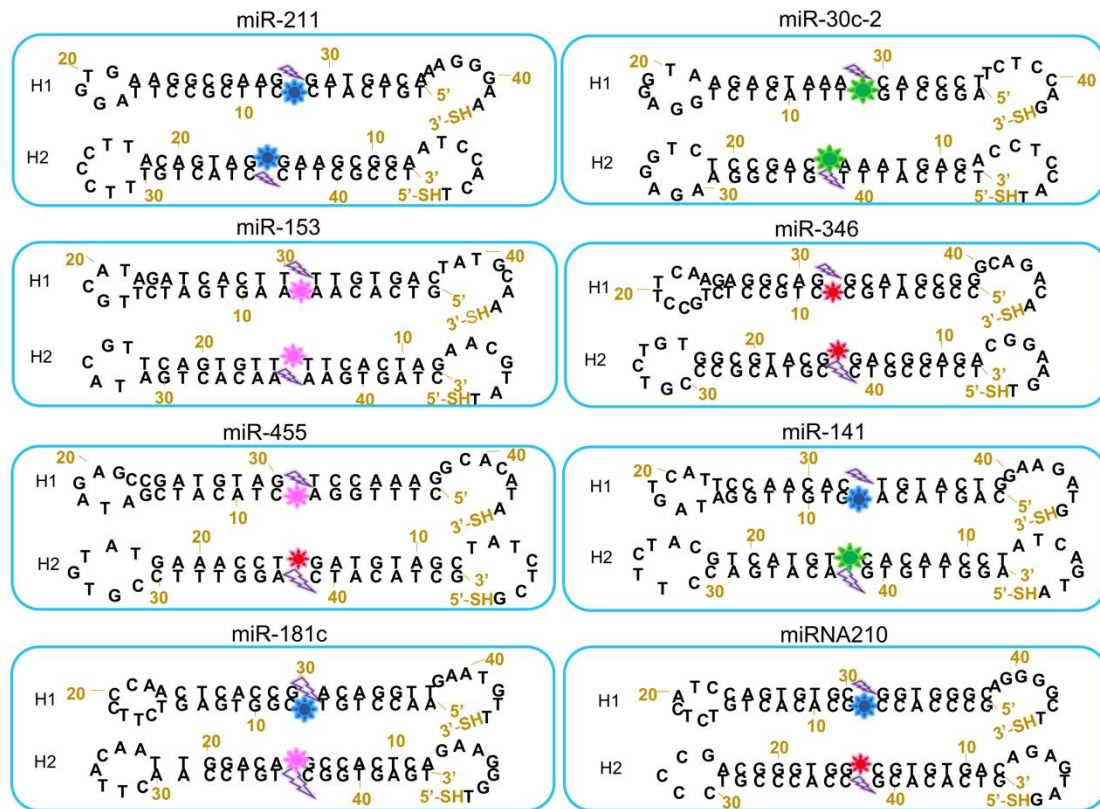


**Fig.S12.** Fluorochrome combinations for eight different miRNAs detection.

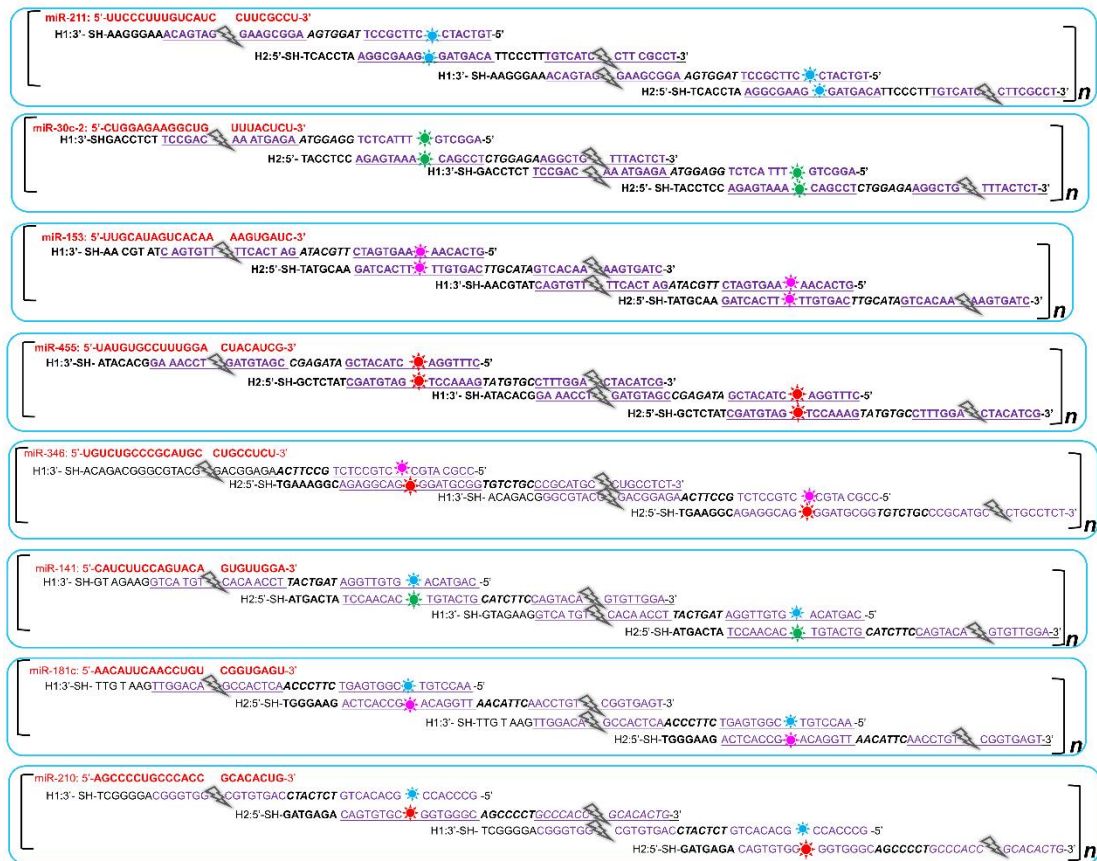
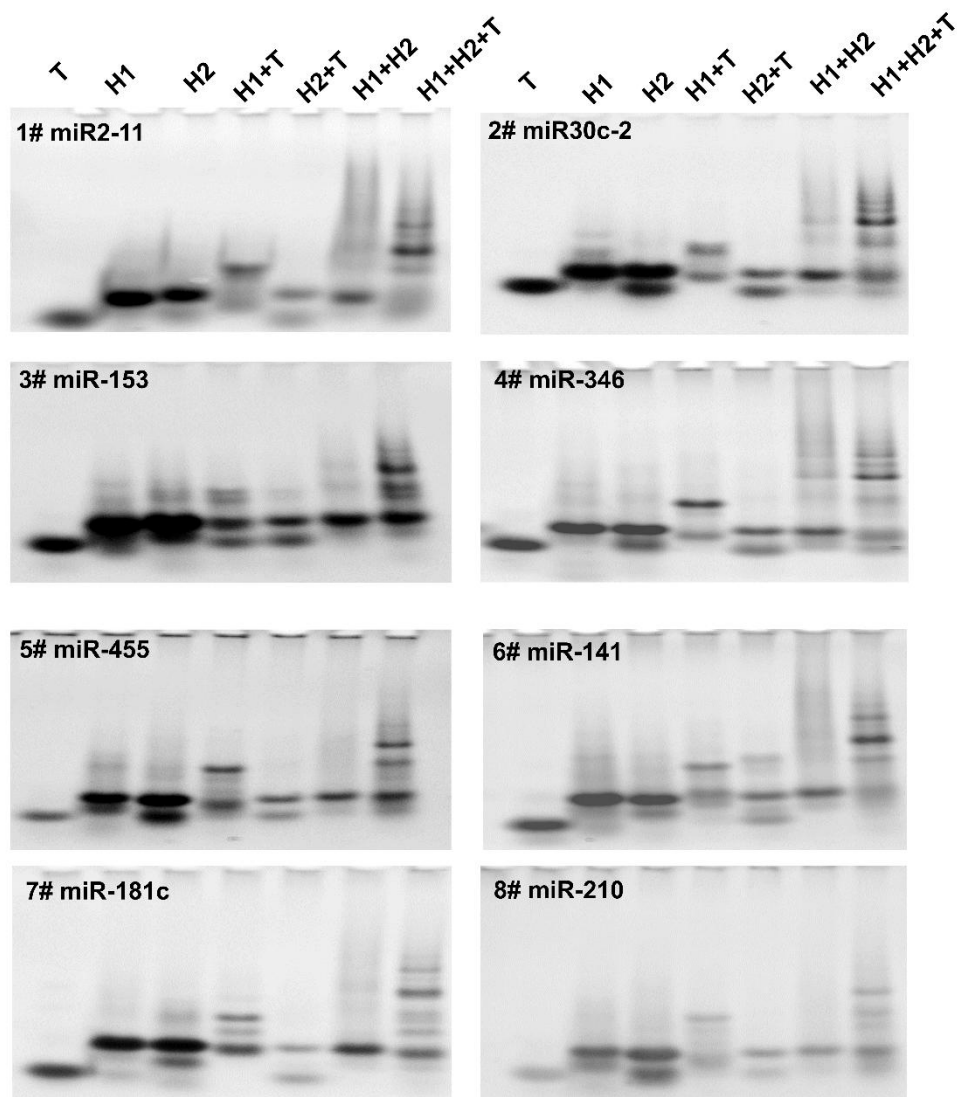
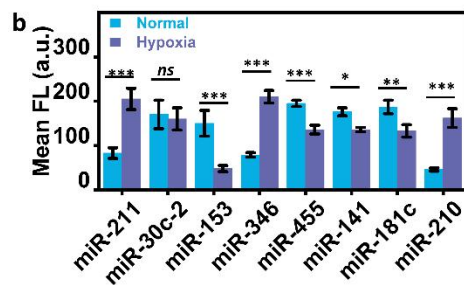
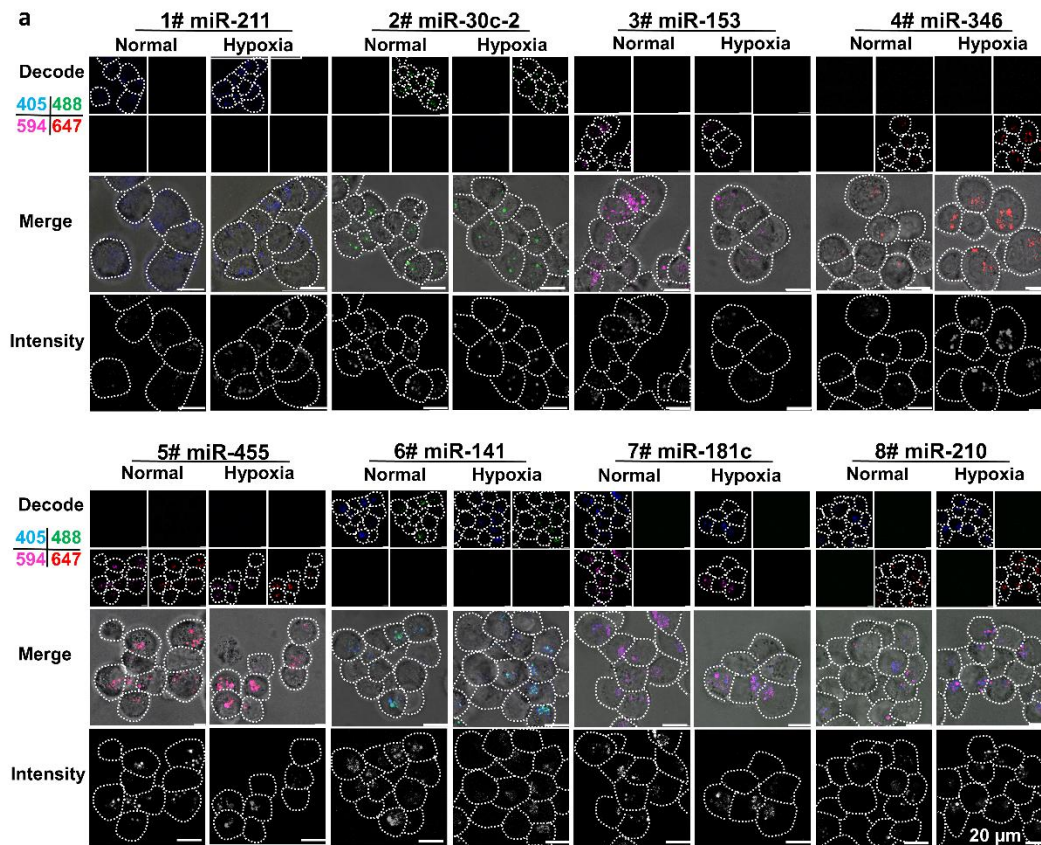


Fig.S13. Multi-HCR barcode extension sequences for the eight miRNAs detection.





**Fig.S14.** Representative native-PAGE electrophoresis for HCR reactions. T: target miRNA; H1: Hairpin 1; H2: Hairpin 2. The sequences were listed in Table S5; the loading concentration of each lane was 2  $\mu$ M.



**Fig.S15.** Multiplexed miRNAs detection separately in hypoxia adaptive signal pathway. (a) Representative CLSM images for the eight hypoxia-induced miRNAs. (b) Mean FL intensity changes for normal and hypoxia treatment.

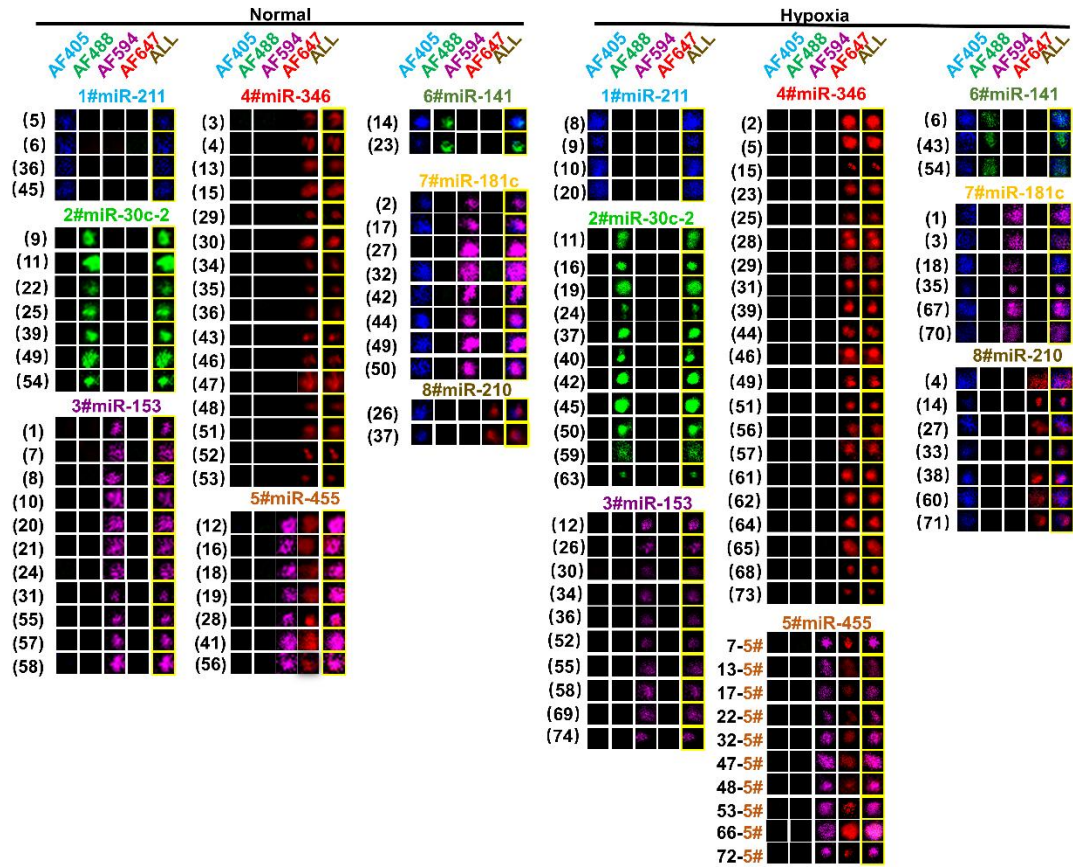


**Fig.S16.** Representative CLSM analysis by channels for decoding the multi-HCR barcodes worked simultaneously in living cells and compared the FL intensity changes in normal and hypoxia-treated Hct116 cells.

## SUPPLEMENTARY TABLES

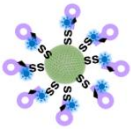




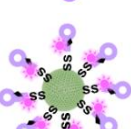
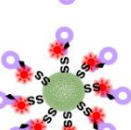
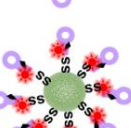
**Table S1.** Sequences used for feasibility analysis of assembling 15 kinds of Multi-HCR barcodes in this work (Take targeting miRNA-155 as a model).

Name	Sequence (5'-3')
miRNA-155	TTAATGCTAATCGTGATAGGGGT
single-base mismatch	UUA AUGCUAAUCGUGAUAGaGGU
two-base mismatch	UUA AUGCUAAUCGUGAUcGaGGU
three-base mismatch	UUA AUGCUAAUCaUGAUcGaGGU
miRNA-155-H1	TAATCGTGATAGGGGTACAGGTCACCCCTATCACGATTAGCATTAA-SH
miRNA-155-H2	HS-GACCTGTACCCCTATCACGATTATTAATGCTAATCGTGATAGGGGT
miRNA-155-H1-405	TAATCGTGAF405ATAGGGGTACAGGTCACCCCTATBHQ1CACGATTAGCATTAA-SH
miRNA-155-H2-405	HS-GACCTGTACCCCTATAF405CACGATTATTAATGCTAATCGTBHQ1GATAGGGGT
miRNA-155-H1-488	TAATCGTGAF488ATAGGGGTACAGGTCACCCCTATBHQ1CACGATTAGCATTAA-SH
miRNA-155-H2-488	HS-GACCTGTACCCCTATAF488CACGATTATTAATGCTAATCGTBHQ1GATAGGGGT
miRNA-155-H1-594	TAATCGTGAF594ATAGGGGTACAGGTCACCCCTATBHQ2CACGATTAGCATTAA-SH
miRNA-155-H2-594	HS-GACCTGTACCCCTAT AF594CACGATTATTAATGCTAATCGTBHQ1GATAGGGGT
miRNA-155-H1-647	TAATCGTG AF647ATAGGGGTACAGGTCACCCCTATBHQ2CACGATTAGCATTAA-SH
miRNA-155-H2-647	HS-GACCTGTACCCCTATAF647CACGATTATTAATGCTAATCGTBHQ2GATAGGGGT

**Table S2.** Multi-HCR chain composition for FL detection in liquid.

Volume ( $\mu\text{L}$ )	1#	2#	3#	4#	5#	6#	7#	8#	9#	10#	11#	12#	13#	14#	15#
miRNA-155-H1-405 (1 $\mu\text{M}$ )	6	0	0	0	6	0	6	0	0	0	2	2	2	0	0
miRNA-155-H2-405 (1 $\mu\text{M}$ )	6	0	0	0	0	6	0	0	0	0	2	2	2	0	3
miRNA-155-H1-488 (1 $\mu\text{M}$ )	0	6	0	0	0	0	0	6	0	0	2	2	0	2	3
miRNA-155-H2-488 (1 $\mu\text{M}$ )	0	6	0	0	6	0	0	0	6	0	2	2	0	2	0
miRNA-155-H1-594 (1 $\mu\text{M}$ )	0	0	6	0	0	6	0	0	0	6	2	0	2	2	0
miRNA-155-H2-594 (1 $\mu\text{M}$ )	0	0	6	0	0	0	0	6	0	0	2	0	2	2	3
miRNA-155-H1-647 (1 $\mu\text{M}$ )	0	0	0	6	0	0	0	0	6	0	0	2	2	2	3
miRNA-155-H2-647 (1 $\mu\text{M}$ )	0	0	0	6	0	0	6	0	0	6	0	2	2	2	0
miRNA-155 (1 $\mu\text{M}$ )	12	12	12	12	12	12	12	12	12	12	12	12	12	12	12
PBS	76	76	76	76	76	76	76	76	76	76	76	76	76	76	76
Total volume ( $\mu\text{L}$ )	100	100	100	100	100	100	100	100	100	100	100	100	100	100	100

**Table S3.** DMSN@H composition used for CLSM detection of miRNA-155 in living cells.

DMSN@H	Structure	HCR probe type
DMSN@H1-405		miRNA-155-H1-405
DMSN@H2-405		miRNA-155-H2-405
DMSN@H1-488		miRNA-155-H1-488
DMSN@H2-488		miRNA-155-H2-488
DMSN@H1-594		miRNA-155-H1-594
DMSN@H2-594		miRNA-155-H2-594
DMSN@H1-647		miRNA-155-H1-647
DMSN@H2-647		miRNA-155-H2-647

**Table S4.** Eight miRNAs' functions in hypoxia-induced signaling pathways reported by former research.

<b>miRNAs</b>	<b>Pathway</b>
miR-211	UPR-PERK-chop <sup>7, 10</sup>
miR-30c-2	UPR-PERK XBP- NF-kB <sup>11</sup>
miR-153	Hypoxia-UPR-IRE1 $\alpha$ -XBP1 -HIF1 $\alpha$ <sup>12</sup>
miR-346	UPR-IRE1 $\alpha$ -XBP-autophagy <sup>13</sup>
miR-455	UPR-ATF6 <sup>14</sup>
miR-141	OXPPOS-mt-COM-V ATP <sup>15</sup>
miR-181c	OXPPOS-mt-COM-1-ROS <sup>16</sup>
miR-210	Hypoxia-OXPPOS mt-COM-IV <sup>17</sup>

**Table S5.** Sequences used for eight miRNAs array analysis in the hypoxia-induced intracellular process.

Name	Sequence (5'-3')
miR-211 (DNA)	TTCCCTTTGTCATCCTTCGCCT
miR-211-H1	TGTCATCCTTCGCCTTAGGTGAAGGCGAAGGATGACAAAGGGAA
miR-211-H2	TCACCTAAGGCGAAGGATGACATTCCTTTGTCATCCTTCGCCT
miR-211-H1-405	TGTCATCAF405CTTCGCCTTAGGTGAAGGCGAAGBHQ1GATGACAAAGGGAA-SH
miR-211-H2-405	HS-TCACCTAAGGCGAAGAF405GATGACATTCCTTTGTCATCBHQ1CTTCGCCT
miR-30c-2 (DNA)	CTGGAGAAGGCTGTTACTCT
miR-30c-2 -H1	AGGCTGTTACTCTGGAGGTAAGAGTAAACAGCCTTCTCCAG
miR-30c-2 -H2	TACCTCCAGAGTAAACAGCCTCTGGAGAAGGCTGTTACTCT
miR-30c-2 -H1-488	AGGCTGAF488TTTACTCTGGAGGTAAGAGTAAABHQ1CAGCCTTCTCCAG-SH
miR-30c-2 -H2-488	HS-ACCTCCAGAGTAAAF488CAGCCTCTGGAGAAGGCTGBHQ1TTTACTCT
miR-153 (DNA)	TTGCATAGTCACAAAAGTGATC
miR-153-H2	GTCACAAAAGTGATCTTGCATAGATCACTTTTGTGACTATGCAA
miR-153-H1	TATGCAA GATCACTTTTGTGACTTGCATAGTCACAAAAGTGATC
miR-153-H1-594	GTCACAAAF594AAGTGATCTTGCATAGATCACTTBHQ2TTGTGACTATGCAA-SH
miR-153-H2-594	SH-TATGCAAGATCACTTAF594TTGTGACTTGCATAGTCACAAABHQ2AAGTGATC
miR-346 (DNA)	TGTCTGCCCGCATGCCTGCCTCT
miR-346-H1	CCGCATGCCTGCCTCTGCCTTCAAGAGGCAGGCATGCGGGCAGACA
miR-346-H2	TGAAGGCAGAGGCAGGCATGCGGTGTCTGCCCGCATGCCTGCCTCT
miR-346-H1-647	CCGCATGCAF647CTGCCTCTGCCTTCAAGAGGCAGBHQ2GCATGCGGGCAGACA-SH
miR-346-H2-647	HS-TGAAGGCAGAGGCAGAF647GCATGCGGTGTCTGCCCGCATGCBHQ2CTGCCTCT
miR-455 (DNA)	TATGTGCCTTTGGACTACATCG
miR-455-H1	CTTTGGACTACATCGATAGAGCCGATGTAGTCCAAAGGCACATA
miR-455-H2	GCTCTATCGATGTAGTCCAAAGTATGTGCCTTTGGACTACATCG
miR-455-H1-594	CTTTGGAAF594CTACATCGATAGAGCCGATGTAGBHQ2TCCAAAGGCACATA-SH
miR-455-H2-647	HS-GCTCTATCGATGTAGAF647TCCAAAGTATGTGCCTTTGGABHQ2CTACATCG
miR-181c (DNA)	AACATTCAACCTGTCGGTGAGT
miR-181c-H1	AACCTGTCGGTGAGTCTTCCAACTCACCAGAGTTGAATGTT
miR-181c-H2	TGGGAAGACTCACCAGAGTTAACATTCAACCTGTCGGTGAGT
miR-181c-H1-405	AACCTGTAF405CGGTGAGTCTTCCAACTCACCGBHQ1ACAGGTTGAATGTT-SH
miR-181c-H2-594	HS-TGGGAAGACTCACCAGAF594ACAGGTTAACATTCAACCTGTBHQ2CGGTGAGT
miR-210 (DNA)	AGCCCCTGCCACCCGACACTG
miR-210-H1	GCCCACCCGACACTGTCTCATCCAGTGTGCGGTGGGCAGGGGCT
miR-210-H2	GATGAGA CAGTGTGCGGTGGGCAGCCCCTGCCACCCGACACTG
miR-210-H1-405	GCCCACCAF405GCACACTGTCTCATCCAGTGTGCBHQ1GGTGGGCAGGGGCT-SH
miR-210-H2-647	HS-GATGAGACAGTGTGCAF647GGTGGGCAGCCCCTGCCACCCBHQ2GCACACTG



**Table S6. Abbreviation List.**

	Abbreviation
microRNA	miRNA
hybridization chain reaction	HCR
fluorescence	FL
rolling circle amplification	RCA
Exchange-Points Accumulation in Nanoscale Topography technique	Exchange-PAINTs
split-probe strategy with multiplexed fluorescence in situ hybridization	split-FISH
Dynamic Light Scattering	DLS
catalyzed hairpin amplification	CHA
biodegradable mesoporous silica nanoparticles	DMSN
Alexa Fluor	AF
attomole	aM
picomole	pM
femtomolar	fM
orthometric multicolor encoded hybridization chain HCR amplifier	multi-HCR
mitochondria	Mito
endoplasmic reticulum	ER
reactive oxygen species	ROS
hairpins	H
glutathione	GSH
Native polyacrylamide gel electrophoresis	Native-PAGE
transmission electron microscope	TEM
dihydroartemisinin	DHA
Cell Counting Kit-8	CCK-8
confocal laser scanning microscope	CLSM
Real-time quantitative PCR	RT-PCR
full width at half maximum	FWHM
quantitative reverse transcriptase polymerase chain reaction	qPCR
cetyltrimethylammoniumtosylate	CTAT
tetraethyl orthosilicate	TEOS
bis3-(triethoxysilyl)propyltetrasulfide	BTESPT
triethanolamine	TEA
L-buthionine sulfoximine	BSO
Förster resonance energy transfer	FRET

## Reference

- 1 K. Jiao, Q. Yan, L. Guo, Z. Qu, S. Cao, X. Chen, Q. Li, Y. Zhu, J. Li, L. Wang, C. Fan, F. Wang, *Angew. Chem.* 2021, **60**, 14438-14445.
- 2 H. M. T. Choi, V. A. Beck, N. A. Pierce, *ACS Nano* 2014, **8**, 4284-4294.
- 3 K. Zhang, Y. Zhang, X. Meng, H. Lu, H. Chang, H. Dong, X. Zhang, *Biomaterials* 2018, **185**, 301-309.
- 4 S. A. Bustin, V. Benes, J. A. Garson, J. Hellemans, J. Huggett, M. Kubista, R. Mueller, T. Nolan, M. W. Pfaffl, G. L. Shipley, J. Vandesompele, C. T. Wittwer, *Clin. Chem.* 2009, **55**, 611-622.
- 5 W.-X. Wang, P. Prajapati, P. T. Nelson, J. E. Springer, *Mol. Neurobiol.* 2020, **57**, 2996-3013.
- 6 Y. Liu, Y. Jiang, M. Zhang, Z. Tang, M. He, W. Bu, *Acc Chem Res* 2018, **51**, 2502-2511.
- 7 T. Kim, C. M. Croce, *Semin. Cancer Biol.* 2021, **75**, 3-4.
- 8 Q. Chen, J. Kang, C. Fu, *Sig. Transduct Target. Ther.* 2018, **3**, 18.
- 9 D. Kessel, J. J. Reiners, *Autophagy* 2020, 1-4.
- 10 N. S. Chitnis, D. Pytel, E. Bobrovnikova-Marjon, D. Pant, H. Zheng, N. L. Maas, B. Frederick, Jake A. Kushner, Lewis A. Chodosh, C. Koumenis, Serge Y. Fuchs, J. A. Diehl, *Mol. Cell* 2012, **48**, 353-364.
- 11 A. E. Byrd, I. V. Aragon, J. W. Brewer, *J. Cell Biol.* 2012, **196**, 689-698.
- 12 H. Liang, J. Xiao, Z. Zhou, J. Wu, F. Ge, Z. Li, H. Zhang, J. Sun, F. Li, R. Liu, C. Chen, *Oncogene* 2018, **37**, 1961-1975.
- 13 (a) J. Guo, Z. Yang, X. Yang, T. Li, M. Liu, H. Tang, *Cancer Lett.* 2018, **413**, 69-81; (b) R. Bartoszewski, J. W. Brewer, A. Rab, D. K. Crossman, S. Bartoszevska, N. Kapoor, C. Fuller, J. F. Collawn, Z. Bebok, *J. Biol. Chem.* 2011, **286**, 41862-41870.
- 14 P. J. Belmont, W. J. Chen, D. J. Thuerauf, C. C. Glembotski, *J. Mol. Cell Cardiol.* 2012, **52**, 1176-1182.
- 15 (a) W. A. Baseler, D. Thapa, R. Jagannathan, E. R. Dabkowski, T. L. Croston, J. M. Hollander, *American Journal of Physiology-Cell Physiology* 2012, **303**, C1244-C1251; (b) J. Bienertova-Vasku, J. Sana, O. Slaby, *Cancer Lett.* 2013, **336**, 1-7.
- 16 (a) S. Das, M. Kohr, B. Dunkerly-Eyring, D. I. Lee, D. Bedja, O. A. Kent, A. K. Leung, J. Henao-Mejia, R. A. Flavell, C. Steenbergen, *Journal of the American Heart Association* 2017, **6**, e004694; (b) C. Jaquenod De Giusti, B. Roman, S. Das, *Frontiers in Physiology* 2018, **9**, 1291.
- 17 (a) F. Elena, R. Anassuya, M. C. Robert, G. Harriet, B. Christine, C. Meredith, D. Cecilia, B. Christopher, B. Francesca, J. L. Li, *PLoS One* 2010, **5**, e10345; (b) D. Sabry, S. E. M. El-Deek, M. Maher, M. A. H. El-Baz, H. M. El-Bader, E. Amer, E. A. Hassan, W. Fathy, H. E. M. El-Deek, *Mol. Cell Biochem.* 2019, **454**, 177-189; (c) Z. Chen, Y. Li, H. Zhang, P. Huang, R. Luthra, *Oncogene* 2010, **29**, 4362-4368.